- Copyright - Il Pensiero Scientifico Editore downloaded by IP 18.97.14.82 Wed, 18 Nov 2026, 17:53:39

Medicina dello Sport, 79 (1), January-March 2026

Distance scaling in volleyball overhead passing: evidence of motor-module reweighting and motor-primitive gain modulation

BOYU SHEN[1], YOUNGSUK KIM[1], XIANGWEI MENG[2], SUKWON KIM[1], BIN ZHU[1]

[1]Department of Physical Education, Jeonbuk National University, Jeonju, Republic of Korea; [2]Department of Sports and Health, Research Center of Sports and Health, Guizhou Medical University, Guiyang, China.

Summary. **Aim**. This study examined how volleyball players scale overhead passing distance by modulating muscle synergy structure. **Methods**. Twenty-four experienced, right-hand–dominant male volleyball players performed overhead passes to targets at 2.5, 5.0, and 7.5 m. Surface electromyography was recorded from 11 upper-limb, trunk, and lower-limb muscles. Muscle synergies were extracted using non-negative matrix factorization. Motor modules were defined as muscle-weighting patterns, whereas motor primitives were defined as the corresponding time-varying activation profiles. Module similarity was assessed using cosine similarity, and distance-dependent changes in motor primitives were evaluated using one-dimensional statistical parametric mapping. **Results**. Three synergies were consistently identified across all passing distances with high reconstruction quality. Increasing passing distance did not require additional synergies. Instead, longer passes were characterized by reweighting of M1–M2 toward greater lower-limb contribution, while M3 remained highly stable. Motor-primitive peak timing was largely preserved across distances, whereas activation amplitudes increased within specific time windows. **Conclusion**. Distance scaling in volleyball overhead passing appears to be achieved primarily through reweighting of existing motor modules and gain modulation of motor primitives rather than through recruitment of additional synergies or temporal reorganization. These findings provide a synergy-based explanation of how players increase passing distance while maintaining temporal coordination and may help coaches design distance-progressive passing drills that preserve technical consistency.

Key words. Volleyball, overhead passing, passing distance, muscle synergies, surface electromyography, non-negative matrix factorization.

Adattamento della distanza nel passaggio sopra la testa nella pallavolo: prove del ribilanciamento dei moduli motori e della modulazione del guadagno delle primitive motorie

Riassunto. Obiettivo. Il presente studio ha esaminato in che modo i giocatori di pallavolo regolano la distanza dei passaggi sopra la testa modulando la struttura delle sinergie muscolari. **Metodi**. Ventiquattro giocatori di pallavolo maschi esperti e destrimani hanno eseguito passaggi sopra la testa verso bersagli situati a 2,5, 5,0 e 7,5 m. È stata registrata l'elettromiografia di superficie su 11 muscoli degli arti superiori, del tronco e degli arti inferiori. Le sinergie muscolari sono state estratte utilizzando la fattorizzazione di matrici non negative. I moduli motori sono stati definiti come modelli di ponderazione muscolare, mentre le primitive motorie sono state definite come i corrispondenti profili di attivazione variabili nel tempo. La somiglianza dei moduli è stata valutata utilizzando la somiglianza cosinusoidale, mentre i cambiamenti delle primitive motorie in funzione della distanza sono stati valutati utilizzando la mappatura parametrica statistica unidimensionale. **Risultati**. Sono state identificate in modo coerente tre sinergie per tutte le distanze di passaggio con un'elevata qualità di ricostruzione. L'aumento della distanza di passaggio non ha richiesto sinergie aggiuntive. Al contrario, i passaggi più lunghi sono stati caratterizzati da una riponderazione di M1–M2 verso un maggiore contributo degli arti inferiori, mentre M3 è rimasto altamente stabile. La tempistica di picco delle primitive motorie è stata in gran parte preservata a tutte le distanze, mentre le ampiezze di attivazione sono aumentate all'interno di specifiche finestre temporali. **Conclusione**. Il ridimensionamento della distanza nel passaggio sopra la testa nella pallavolo sembra essere ottenuto principalmente attraverso la riponderazione dei moduli motori esistenti e la modulazione del guadagno delle primitive motorie piuttosto che attraverso il reclutamento di sinergie aggiuntive o la riorganizzazione temporale. Questi risultati forniscono una spiegazione basata sulle sinergie di come i giocatori aumentino la distanza di passaggio mantenendo la coordinazione temporale e possono aiutare gli allenatori a progettare esercizi di passaggio con distanza progressiva che preservino la coerenza tecnica.

Parole chiave. Pallavolo, passaggio sopra la testa, distanza di passaggio, sinergie muscolari, elettromiografia di superficie, fattorizzazione di matrici non negative.

- Copyright - Il Pensiero Scientifico Editore downloaded by IP 18.97.14.82 Wed, 18 Nov 2026, 17:53:39

Introduction

In volleyball, overhead passing (setting) is a core technical skill that links reception and defense to attack and strongly influences offensive tempo and tactical options[1,2]. During match play, setters must execute overhead passes across a wide range of distances and tempos, from short, fast sets to long, court-covering adjustment passes[3,4]. As passing distance and spatial constraints increase, task difficulty rises: players must maintain precise hand–ball interaction and a stable release while generating sufficient ball speed and an appropriate flight trajectory[5]. This creates a demanding motor-control problem because the neuromuscular system must increase mechanical output without compromising the accuracy and stability of ball release.

Biomechanical studies have begun to describe distance scaling in overhead passing at the kinematic and kinetic levels, suggesting that longer passes involve greater lower-limb drive and trunk contribution[5,6]. These findings indicate that distance scaling in overhead passing is a whole-body task rather than an isolated upper-limb action. However, these macroscopic observations leave a key question unresolved: how is muscle recruitment coordinated to meet higher distance demands while preserving control at release? From a motor-control perspective, distance scaling requires whole-body coordination, because players must control release parameters at ball release while coordinating lower-limb, trunk, and upper-limb actions[5,7,8]. Therefore, understanding distance scaling in overhead passing requires further examination of the neuromuscular control mechanisms underlying these biomechanical adaptations.

Muscle synergy analysis provides a useful framework for examining this motor-control problem. Human movement is characterized by a high degree of redundancy, because a given task goal can be achieved through multiple combinations of joint motion and muscle activation[9,10]. Muscle synergies have been proposed as one way in which the neuromuscular system organizes this redundancy into lower-dimensional coordination patterns[11,12]. Within this framework, muscle weightings represent the relative contribution of each muscle within a motor module, whereas time-varying activation profiles, or motor primitives, indicate when and to what extent each module is activated during movement[13,14]. Previous distance-dependent muscle synergy research in basketball shooting showed that increasing distance can alter synergy patterns without changing the number of synergies[15]. However, volleyball overhead passing imposes different task constraints, because players must redirect the ball during a brief hand–ball contact phase rather than grasping and releasing it after possession[16]. Therefore, findings from distance-dependent shooting tasks cannot be directly generalized to volleyball overhead passing, and it remains unclear how players scale passing distance through modular neuromuscular coordination.

Therefore, this study aimed to clarify the neuromuscular control mechanisms underlying distance scaling in volleyball overhead passing using muscle synergy analysis. Specifically, we compared the number of muscle synergies, motor-module composition, muscle weightings, and motor primitives across different passing distances. We hypothesized that distance scaling would be achieved primarily through selective changes in muscle weightings and modulation of motor primitives, rather than through changes in the number of synergies.

Methods

Participants

Twenty-four experienced young adult male volleyball players with right-hand dominance were recruited for this study. Participants were required to have completed at least five years of systematic volleyball training and to be currently engaged in regular university- or club-level training. The sample included players from different playing positions, because overhead passing is a fundamental volleyball skill required across positions. Participant characteristics were as follows: age, 21.3 ± 3.8 years; height, 1.85 ± 0.17 m; body mass, 74.4 ± 7.3 kg; and systematic volleyball training experience, 8.0 ± 2.2 years. The sample size was determined with reference to previous sport-specific muscle synergy studies, in which similar or smaller sample sizes have commonly been used. Accordingly, the present sample of 24 participants was considered appropriate for this within-subject muscle synergy analysis. All participants reported no musculoskeletal injuries within the six months preceding data collection. Written informed consent was obtained from all participants prior to testing. The study protocol was approved by the Institutional Review Board of Jeonbuk National University (JBNU2024-09-015-002).

Experimental procedure

Before formal testing, the investigators provided standardized instructions regarding the experimental protocol and movement requirements. Participants then completed a 10-min standardized warm-up and performed practice trials to familiarize themselves with the task. A volleyball coach with extensive coaching experience delivered consistent tosses, and participants were instructed to perform an overhead pass of the incoming ball to a predefined target ar-

- Copyright - Il Pensiero Scientifico Editore downloaded by IP 18.97.14.82 Wed, 18 Nov 2026, 17:53:39

ea, which consisted of a circular ring positioned at a height of 2.53 m with a diameter of 1.0 m[5]. Tosses were delivered from a consistent location and trajectory to ensure comparable incoming ball height and direction across trials. Three passing-distance conditions were tested: short (2.5 m), medium (5.0 m), and long (7.5 m)[5]. A trial was considered successful when the ball passed through the ring. Unsuccessful trials were excluded and repeated until three successful trials were obtained for each passing-distance condition. A 1-min rest interval was provided between trials to minimize fatigue accumulation.

Data collection

Surface electromyography (EMG) signals were recorded using 11 wireless EMG sensors (Trigno Avanti; Delsys, Natick, MA, USA) at 1200 Hz from the following muscles: flexor carpi radialis (FCR), extensor carpi ulnaris (ECU), biceps brachii (BB), triceps brachii (TB), anterior deltoid (AD), rectus abdominis (RA), erector spinae (ES), rectus femoris (RF), biceps femoris (BF), lateral gastrocnemius (GL), and tibialis anterior (TA). EMG was collected from the dominant (right) side. Prior to sensor placement, hair over the electrode sites was shaved and the skin was cleaned with alcohol to reduce impedance[17]. After sensor placement, EMG signal quality was checked during quiet standing and task-specific practice trials. Sensors were repositioned when unstable contact, excessive baseline noise, or obvious motion artifacts were observed.

Fifty-seven 14-mm reflective markers were placed on the participant's skin in accordance with a previously established protocol, as shown in figure 1[18]. In addition, five hemispherical reflective markers were attached to the ball surface to enable three-dimensional tracking of ball motion during overhead passing without interfering with performance[5]. Three-dimensional kinematic data were captured using a motion-capture system comprising 13 infrared cameras

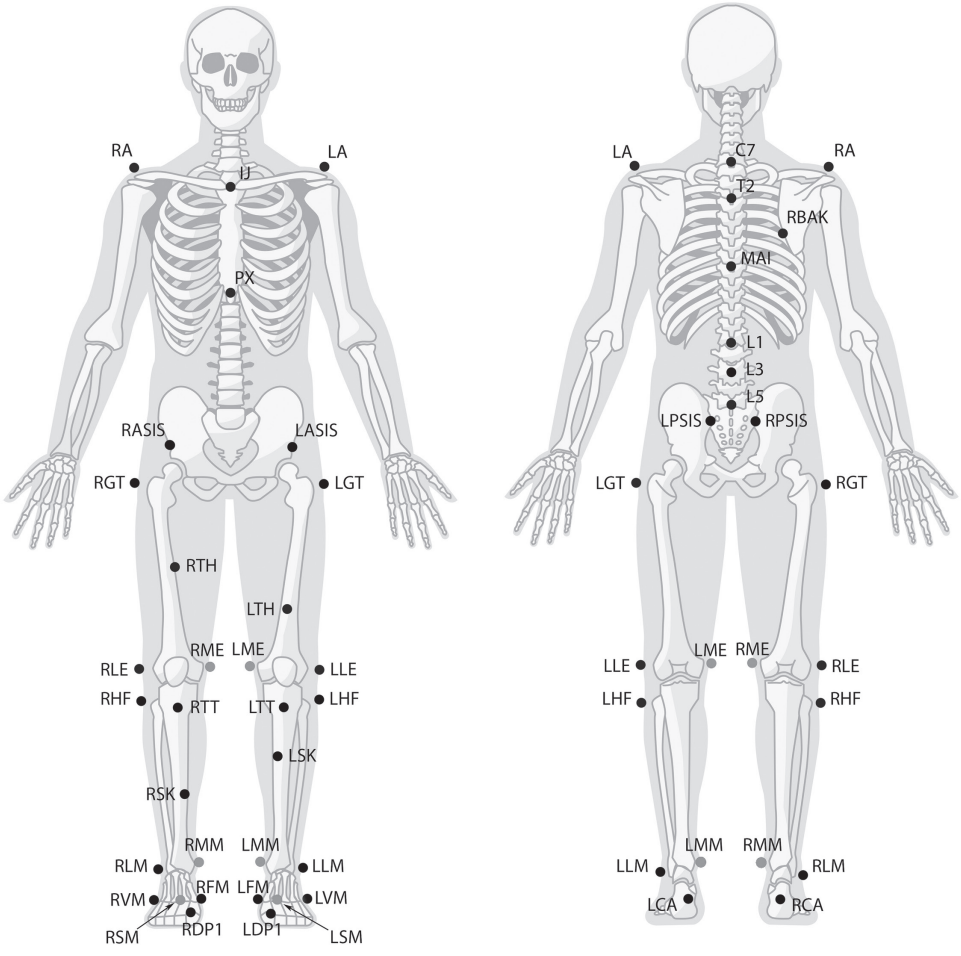

Figure 1. Marker attachment location.

- Copyright - Il Pensiero Scientifico Editore downloaded by IP 18.97.14.82 Wed, 18 Nov 2026, 17:53:39

(Prime 17W; OptiTrack, NaturalPoint Inc., Corvallis, OR, USA) at 240 Hz. A static calibration trial was collected prior to the dynamic trials. Kinematic and EMG data were synchronized and recorded using Motive 2.2.0 (OptiTrack, NaturalPoint Inc.).

Data processing and analysis

All raw data were imported into Visual3D x64 v2024.10.4 (C-Motion, Rockville, MD, USA) for preprocessing. A whole-body multi-segment rigid-body model and a volleyball rigid-body model were constructed based on the reflective marker sets. Marker trajectories were low-pass filtered using a fourth-order, zero-lag (bidirectional) Butterworth filter with a cutoff frequency of 20 Hz to facilitate identification of key movement events[19]. Previous work has shown that the main phase of overhead passing – from ball contact to ball release – lasts approximately 116–136 ms from short to long passing distances[6]. Therefore, ball release was defined as time zero (t = 0) and was identified from the ball kinematics as the instant when the ball entered free flight, operationalized as the time point at which the ball's vertical acceleration approached gravitational acceleration (≈ −9.81 $m \cdot s^{-2}$ in the laboratory vertical axis)[6]. The detected release event was visually inspected in Visual3D for each trial to ensure correct event identification. EMG data from 250 ms before to 80 ms after ball release (−250 to +80 ms) were extracted for muscle synergy analysis, covering the late preparatory phase and the follow-through phase relative to release.

Raw EMG signals were processed in Visual3D. Signals were band-pass filtered using a fourth-order zero-lag Butterworth filter with cutoff frequencies of 20–450 Hz[15]. EMG envelopes were then obtained using the Visual3D Moving_RMS command with a 100-ms centered window and subsequently low-pass filtered at 6 Hz using a fourth-order zero-lag Butterworth filter[15]. For each participant, each muscle was normalized to the maximum envelope value observed across all successful trials and passing-distance conditions[20]. All preprocessing steps were completed before time normalization. For each participant and passing-distance condition, the three successful trials were time-normalized and averaged point by point before muscle synergy extraction to obtain a representative condition-specific EMG profile.

The processed EMG signals within the analysis window from −250 to +80 ms relative to ball release were then time-normalized to 101 data points for each successful trial. For each participant and passing-distance condition, time-normalized EMG signals were averaged across successful trials to obtain a single representative EMG profile for each muscle. The resulting trial-averaged EMG matrix was exported to MATLAB (R2025b; The MathWorks Inc., Natick, MA, USA) and used as the input for NNMF.

Non-negative matrix factorization (NNMF)[21] was applied to the assembled EMG matrix $E_{m\times t}$ *as*:

$$E_{m\times t} = M_{m\times n} P_{n\times t} + R_{m\times t}$$

where n denotes the number of muscle synergies; $M_{m\times n}$ is the motor module matrix (each column represents a synergy and each element indicates the relative contribution of a muscle); $P_{n\times t}$ is the motor primitive matrix (each row describes the time-varying activation profile of the corresponding synergy); and $R_{m\times t}$ is the residual matrix.

Because NNMF solutions can depend on the initial random values, NNMF was repeated 20 times for each participant and passing-distance condition using different random initializations. This procedure was used to reduce the risk of convergence to local minima, and the solution with the smallest reconstruction error was retained[15].

To determine the number of synergies, variance accounted for (VAF) was computed[22] as:

$$\mathrm{VAF} = 1 - \frac{||E - M * P||F^2}{||E||F^2}$$

Where $||\cdot||F$ denotes the Frobenius norm. E denotes the normalized original EMG matrix, and $M*P$ represents the EMG matrix reconstructed by the synergy model.

For each participant and passing-distance condition, total VAF was computed for different numbers of synergies from n = 1–11 (figure 2). A total VAF threshold of 0.95 has been commonly used as a high reconstruction criterion in previous NNMF-based muscle synergy studies[23]. Because reconstruction accuracy generally increases with the number of extracted synergies, the number of synergies was selected as the minimum n that satisfied the predefined VAF criterion across all passing-distance conditions, thereby balancing reconstruction accuracy with model parsimony[22]. When n = 3, VAF values were 0.984 ± 0.007 for 2.5 m, 0.977 ± 0.007 for 5.0 m, and 0.978 ± 0.008 for 7.5 m, all exceeding the threshold. Therefore, n = 3 was fixed for all passing-distance conditions (supplementary table S1).

To obtain representative synergy patterns, motor-module vectors were normalized to unit length and classified across the 24 participants using k-means clustering within each passing-distance condition (K = 3)[24]. Clustering was repeated 50 times with different random centroid initializations, and the solution with the highest silhouette score was selected[15]. The centroid of each cluster was used as the representative motor module, and the associated motor primitives were averaged according to the corresponding cluster labels. Because NNMF-de-

- Copyright - Il Pensiero Scientifico Editore downloaded by IP 18.97.14.82 Wed, 18 Nov 2026, 17:53:39

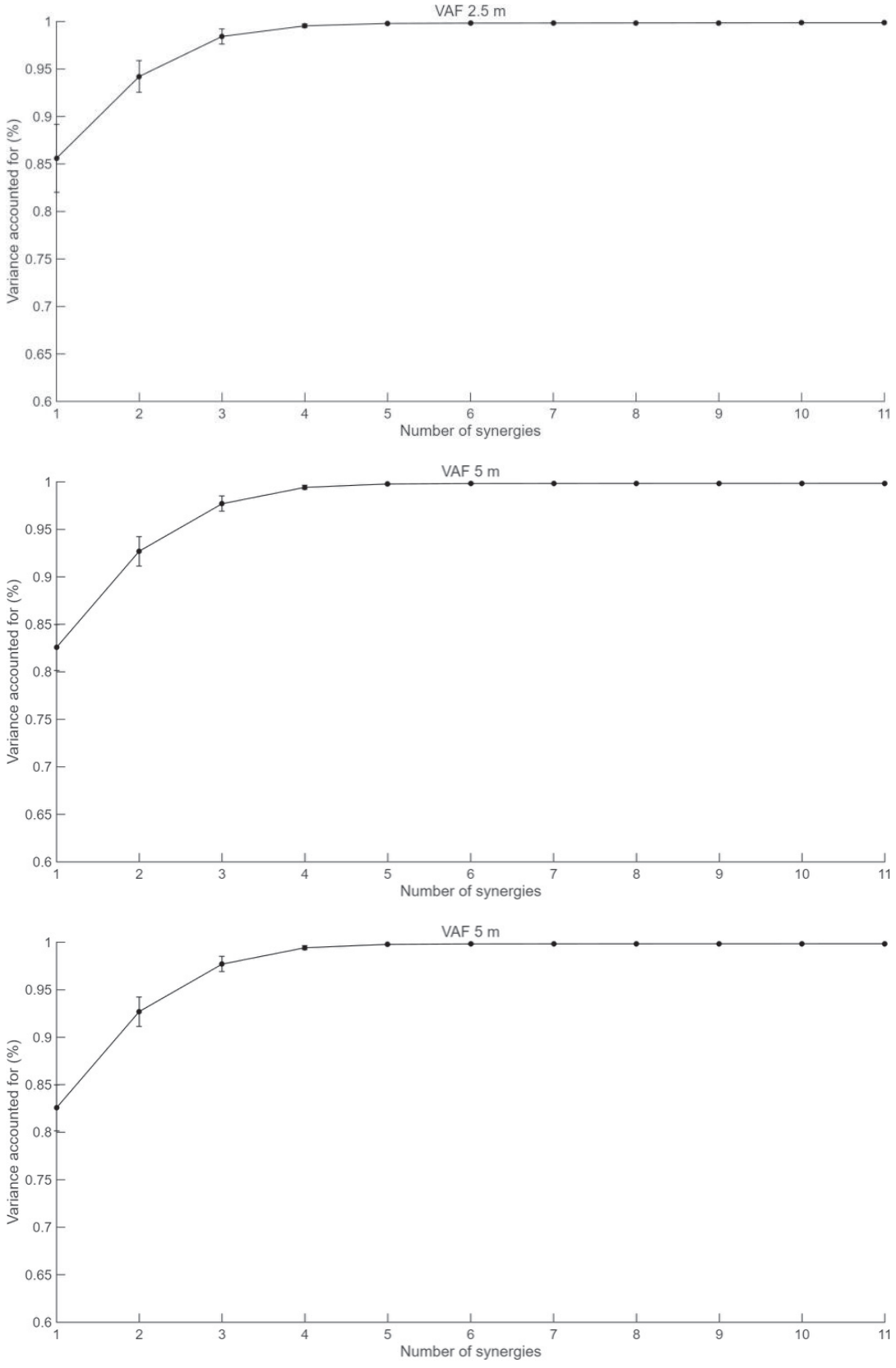

Figure 2. Mean VAF and standard deviation across different numbers of muscle synergies for the three passing distances.

- Copyright - Il Pensiero Scientifico Editore downloaded by IP 18.97.14.82 Wed, 18 Nov 2026, 17:53:39

rived modules have an arbitrary order, cluster assignment was used to resolve label switching across participants[25]. Representative modules were then matched across distance conditions by maximizing cosine similarity between cluster centroids[25]. This procedure yielded distance-specific representative patterns with consistent labels for subsequent comparisons.

Statistical analysis

To evaluate structural similarity of motor modules across passing-distance conditions, cosine similarity (CS) was computed between motor-module weighting vectors[26]. CS ≥ 0.90 was adopted as the threshold for high similarity[27]. To ensure consistent module labeling across conditions, modules were matched by maximizing CS before comparison[25]. When a module pair showed low similarity across distances (CS < 0.90), post hoc muscle-weighting comparisons were performed to identify the specific muscles contributing to module reweighting. Normality of paired differences was assessed before testing; paired-samples t-tests or Wilcoxon signed-rank tests were used as appropriate. P-values were adjusted using the Holm–Bonferroni procedure across the 11 muscle comparisons within each module-distance pair. Effect sizes were reported as Cohen's dz for paired t-tests and r for Wilcoxon tests.

To examine distance-dependent changes in the temporal domain of motor primitives, one-dimensional statistical parametric mapping (SPM1d) was used to perform a one-way repeated-measures ANOVA (RM-ANOVA) on motor primitives across the three passing-distance conditions[28]. Significant main effects were identified from the SPM(F) trajectory. When a significant main effect of distance was detected, Bonferroni-corrected post hoc SPM(t) pairwise comparisons were performed, with the significance level adjusted to $\alpha = 0.017$[15]. For each significant SPM cluster, the critical threshold, exact time interval, and cluster-level p-value were reported. Effect sizes were computed point-wise and reported as the mean value within each significant cluster, with partial eta squared (ηp^2) used for SPM(F) results and Cohen's dz used for post hoc SPM(t) comparisons. All statistical analyses were conducted in MATLAB.

Results

Motor module characteristics across overhead passing distances

Figures 3-5 illustrate the motor modules and motor primitives extracted under the 2.5, 5.0, and 7.5 m passing conditions. Three motor modules (M1–M3) were consistently identified across distances, each showing distinct muscle-weighting patterns. Cosine similarity analysis showed that most motor modules were highly similar across passing distances (CS ≥ 0.90; table 1). However, M1 and M2 showed low similarity between the 2.5 m and 7.5 m conditions (M1: CS = 0.8256; M2: CS = 0.7379), indicating distance-dependent reweighting of these two modules. Therefore, post hoc muscle-weighting comparisons were restricted to M1 and M2 between the 2.5 m and 7.5 m conditions.

For M1, after Holm–Bonferroni correction, the 2.5 m condition showed significantly greater weightings for BB and AD, whereas the 7.5 m condition showed significantly greater weightings for RF and BF (figure 6; table 2; detailed post hoc statistics, including mean differences and 95% confidence intervals, are provided in supplementary table S2). These results indicate that M1 shifted from a more upper-limb-dominant pattern at 2.5 m toward greater lower-limb contribution at 7.5 m.

For M2, after Holm–Bonferroni correction, the 2.5 m condition showed significantly greater weightings for FCR, ECU, TB, and AD, whereas the 7.5 m condition showed significantly greater weightings for RF, BF, and GL (figure 6; table 2). This pattern indicates a more pronounced distance-dependent reweighting of M2, characterized by reduced upper-limb contribution and increased lower-limb contribution during long-distance passing.

Motor primitive characteristics across overhead passing distances

Motor primitive P1 showed dominant activation during the early phase of the movement (figure 7, P1). SPM1d RM-ANOVA revealed a significant main effect of passing distance from 0.0% to 45.0% of the normalized movement cycle. Post hoc SPM(t) comparisons showed progressively greater P1 activation with increasing passing distance, with significant differences mainly occurring during the early activation window.

Motor primitive P2 showed dominant activation during the middle phase of the movement (figure 7, P2). A significant main effect of passing distance was observed from 26.0% to 76.0% of the normalized movement cycle. Post hoc SPM(t) comparisons showed that P2 activation increased with passing distance, with the 7.5 m condition showing greater activation than both the 2.5 m and 5.0 m conditions across substantial portions of the middle activation window.

Motor primitive P3 showed dominant activation during the late phase of the movement (figure 7, P3). A significant main effect of passing distance was ob-

- Copyright - Il Pensiero Scientifico Editore downloaded by IP 18.97.14.82 Wed, 18 Nov 2026, 17:53:39

served from 62.0% to 100.0% of the normalized movement cycle. Post hoc SPM(t) comparisons indicated greater late-phase activation as passing distance increased, particularly in the 7.5 m condition.

Detailed SPM results, including critical thresholds, exact significant time intervals, cluster-level p-values, and mean effect sizes within significant clusters, are provided in table 3. Overall, P1–P3 showed dis-

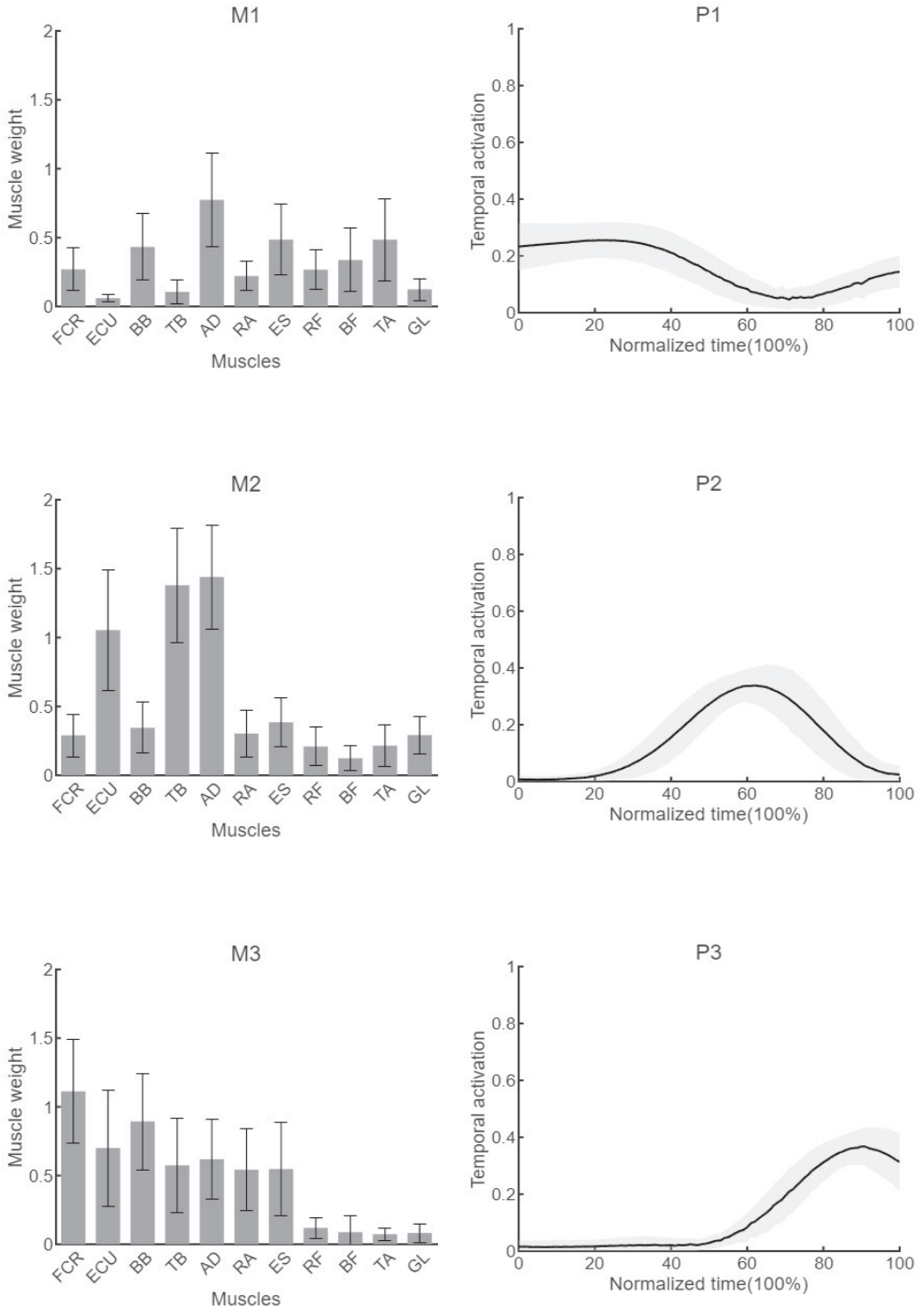

Figure 3. Motor modules (M1–M3) and motor primitives (P1–P3) extracted for the 2.5 m passing condition. The left panels show muscle weightings (bars: mean; error bars: SD), and the right panels show the corresponding motor primitives (black line: mean; shaded area: SD). Time is normalized to 0–100% of the analysis window (–250 to +80 ms relative to ball release).

- Copyright - Il Pensiero Scientifico Editore downloaded by IP 18.97.14.82 Wed, 18 Nov 2026, 17:53:39

tance-dependent amplitude increases within their dominant activation windows, whereas the temporal sequence of the three primitives remained consistent across passing distances.

Discussion

Consistent with our hypothesis, the present results demonstrate that distance scaling in volleyball over-

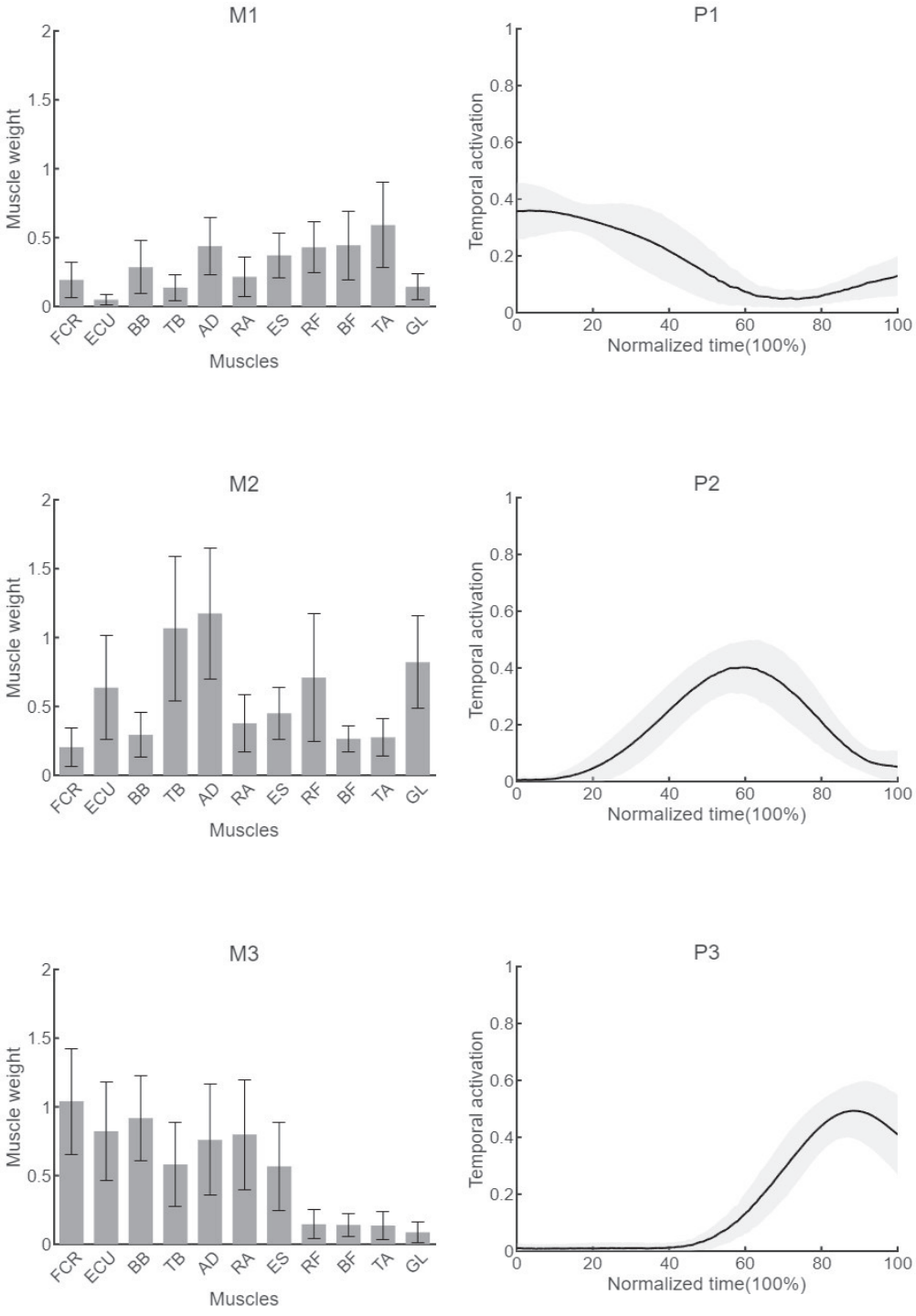

Figure 4. Motor modules (M1–M3) and motor primitives (P1–P3) extracted for the 5.0 m passing condition. The left panels show muscle weightings (bars: mean; error bars: SD), and the right panels show the corresponding motor primitives (black line: mean; shaded area: SD). Time is normalized to 0–100% of the analysis window (–250 to +80 ms relative to ball release).

- Copyright - Il Pensiero Scientifico Editore downloaded by IP 18.97.14.82 Wed, 18 Nov 2026, 17:53:39

head passing occurs without changes in the number of muscle synergies. Three synergies were sufficient to reconstruct EMG activity across all passing distances, and no additional synergies emerged as distance increased. However, distance-related changes were evident in both the spatial and temporal components of the synergy structure. Specifically, M1 and M2 showed distance-dependent reweighting between

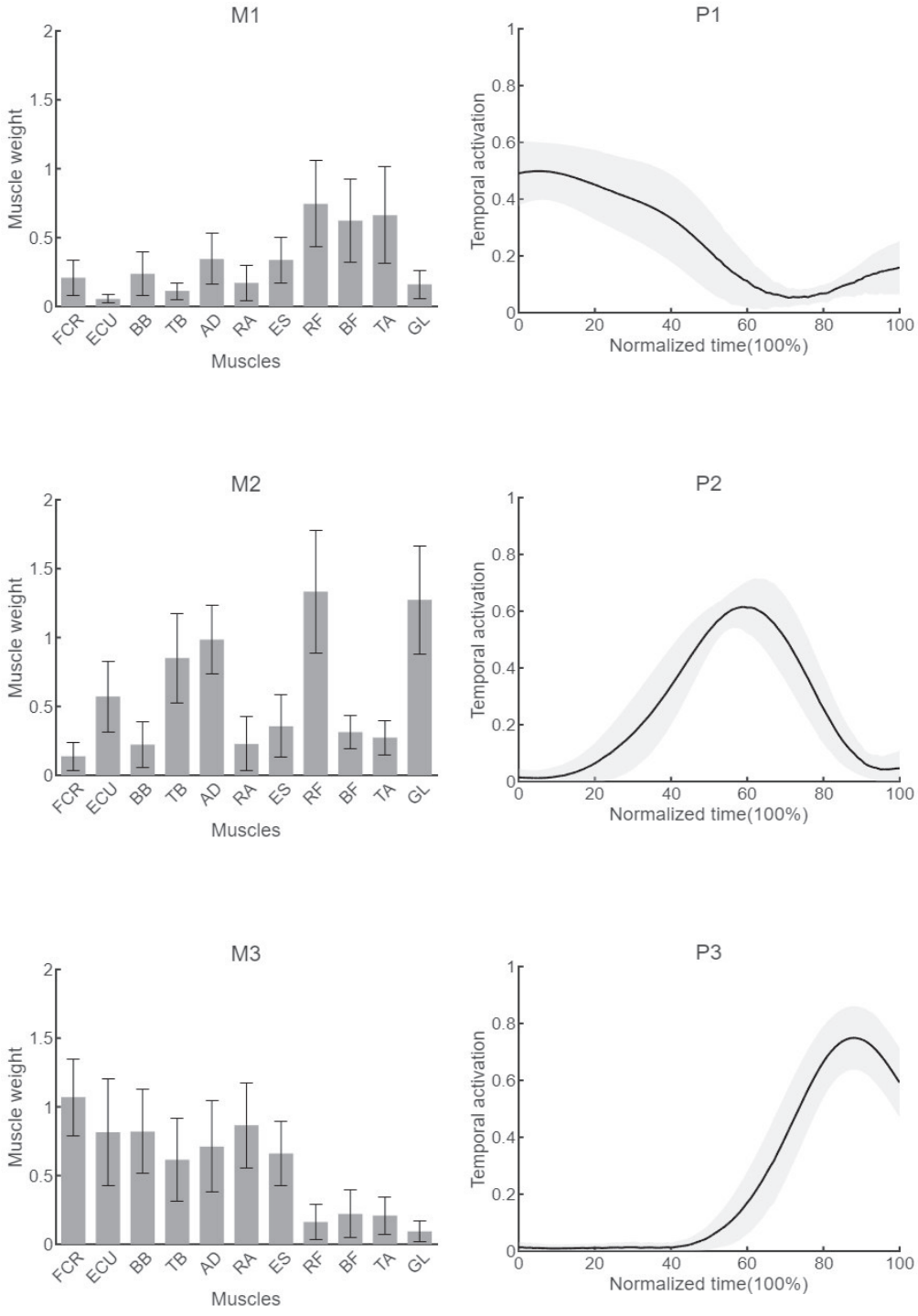

Figure 5. Motor modules (M1–M3) and motor primitives (P1–P3) extracted for the 7.5 m passing condition. The left panels show muscle weightings (bars: mean; error bars: SD), and the right panels show the corresponding motor primitives (black line: mean; shaded area: SD). Time is normalized to 0–100% of the analysis window (–250 to +80 ms relative to ball release).

- Copyright - Il Pensiero Scientifico Editore downloaded by IP 18.97.14.82 Wed, 18 Nov 2026, 17:53:39

Table 1. Cosine similarity of motor modules across passing distances.

Distance	Cosine similarity		
	M1	M2	M3
2.5 m and 5.0 m	0.9346	0.9163	0.9896
2.5 m and 7.5 m	0.8256*	0.7379*	0.9828
5.0 m and 7.5 m	0.9643	0.9369	0.9958

Note. Values closer to 1 indicate greater similarity between motor-module weighting vectors. CS ≥ 0.90 was defined as high similarity. * indicates low similarity below the predefined threshold (CS < 0.90).

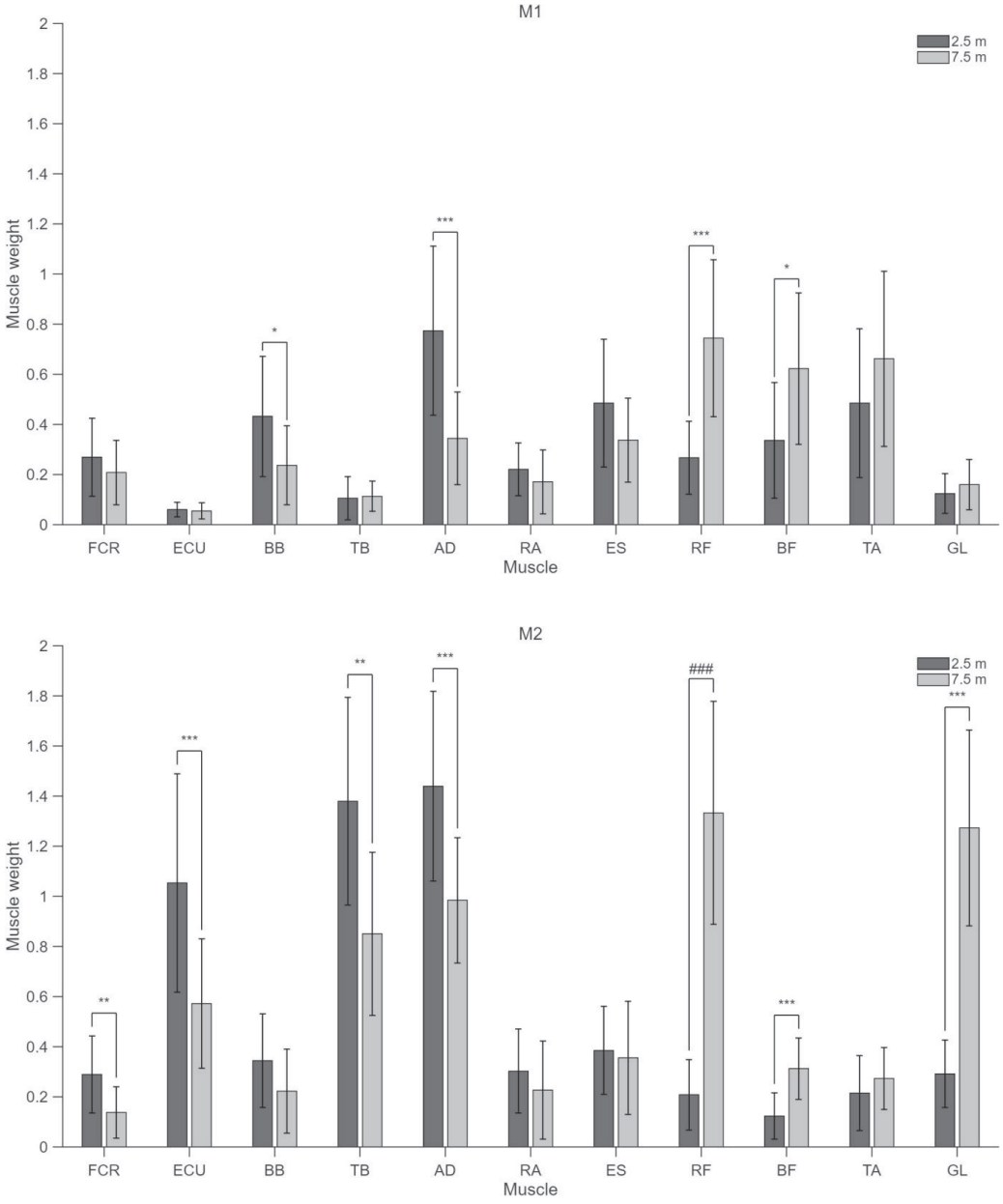

Figure 6. Post hoc comparisons of muscle weightings in motor module 1 (M1) and motor module 2 (M2) between the 2.5 m and 7.5 m passing conditions. Bars represent mean ± SD; black = 2.5 m and gray = 7.5 m. Significance markers indicate Holm–Bonferroni-adjusted p-values. * p ≤ 0.05, ** p ≤ 0.01, *** p ≤ 0.001. #, ##, and ### denote results from Wilcoxon signed-rank tests with the same adjusted p-value thresholds.

- Copyright - Il Pensiero Scientifico Editore downloaded by IP 18.97.14.82 Wed, 18 Nov 2026, 17:53:39

Table 2. Post hoc comparisons of muscle weightings for motor modules showing low cosine similarity.

Module	Muscle	2.5 m mean ± SD	7.5 m mean ± SD	Test	Adjusted p	Effect size
M1	BB	0.432 ± 0.240	0.237 ± 0.158	paired t-test	0.024	dz = –0.676
M1	AD	0.774 ± 0.338	0.344 ± 0.184	paired t-test	<0.001	dz = –1.101
M1	RF	0.267 ± 0.145	0.744 ± 0.313	paired t-test	<0.001	dz = 1.511
M1	BF	0.336 ± 0.231	0.623 ± 0.302	paired t-test	0.017	dz = 0.716
M2	FCR	0.289 ± 0.154	0.138 ± 0.102	paired t-test	0.004	dz = –0.779
M2	ECU	1.054 ± 0.436	0.572 ± 0.257	paired t-test	<0.001	dz = –1.087
M2	TB	1.380 ± 0.415	0.851 ± 0.325	paired t-test	0.001	dz = –0.912
M2	AD	1.439 ± 0.379	0.985 ± 0.250	paired t-test	<0.001	dz = –1.056
M2	RF	0.208 ± 0.140	1.333 ± 0.445	Wilcoxon	<0.001	r = 0.875
M2	BF	0.123 ± 0.092	0.313 ± 0.122	paired t-test	<0.001	dz = 1.426
M2	GL	0.292 ± 0.135	1.273 ± 0.390	paired t-test	<0.001	dz = 2.338

Note. Only muscles that remained significant after Holm–Bonferroni correction are shown. Adjusted p-values were obtained using the Holm–Bonferroni procedure across the 11 muscle-weighting comparisons within each module. Cohen's dz was calculated as 7.5 m minus 2.5 m; therefore, negative dz values indicate greater weightings in the 2.5 m condition, whereas positive dz values indicate greater weightings in the 7.5 m condition. For the Wilcoxon signed-rank test, r indicates the non-parametric effect size.

the 2.5 m and 7.5 m conditions, shifting from greater upper-limb contribution at the shorter distance toward greater lower-limb contribution at the longer distance. In the temporal domain, motor-primitive peak timing (P1–P3) was largely preserved, whereas activation amplitudes increased with distance within each primitive's dominant time window. These findings suggest that, within the recorded muscle set and present task constraints, distance scaling was mainly expressed through motor-module reweighting and motor-primitive gain modulation rather than through recruitment of additional synergies.

This interpretation should be considered within the broader framework of modular motor control. Muscle synergy analysis has been widely used to describe how the neuromuscular system organizes the activity of multiple muscles into a smaller set of functional modules or low-dimensional coordination patterns[12,29]. However, synergies extracted from EMG decomposition algorithms should be interpreted cautiously as coordination patterns rather than as direct proof of fixed neural modules, because low-dimensional EMG structure may also reflect task, biomechanical, or methodological constraints[30,31]. Within this framework, the present results indicate that experienced volleyball players preserved a low-dimensional coordination structure while adjusting the relative contribution and activation intensity of existing modules. This provides a more nuanced interpretation of distance scaling: longer passes did not require a new coordination architecture, but rather a redistribution and amplification of existing coordination components.

The greater lower-limb contribution in M1–M2 during long-distance passing indicates a shift from an arm-dominant strategy to a more integrated whole-body strategy as distance demands increased. This agrees with previous biomechanical evidence showing greater lower-limb drive, trunk involvement, and inter-joint energy transfer during longer overhead passes[5,6]. In contrast, the preserved structure of M3 across distances may indicate that the terminal control component of overhead passing remained stable. Previous biomechanical analysis of the volleyball overhead pass emphasized the importance of the wrist flexor stretch-shortening cycle and the elbow-to-wrist kinetic chain during the ball-contact and push phases, suggesting that stable distal coordination is important for effective ball release control[16]. Therefore, distance scaling appears to involve selective reweighting of force-generating modules while preserving a relatively stable terminal-control module.

A key mechanistic question concerns why distance effects were expressed predominantly as amplitude scaling rather than changes in motor-primitive timing. In the present data, the peak timing and temporal ordering of P1–P3 appeared largely preserved across distances, whereas distance effects were expressed mainly as increases in activation amplitude within their dominant activation windows. This pattern is compatible with muscle synergy models in which changes in task demands can be accommodated by modulating synergy recruitment strength or amplitude coefficients without necessarily generating new coordination structures[32,33]. The brief hand–ball contact window, reported to be approximately 116–136

- Copyright - Il Pensiero Scientifico Editore downloaded by IP 18.97.14.82 Wed, 18 Nov 2026, 17:53:39

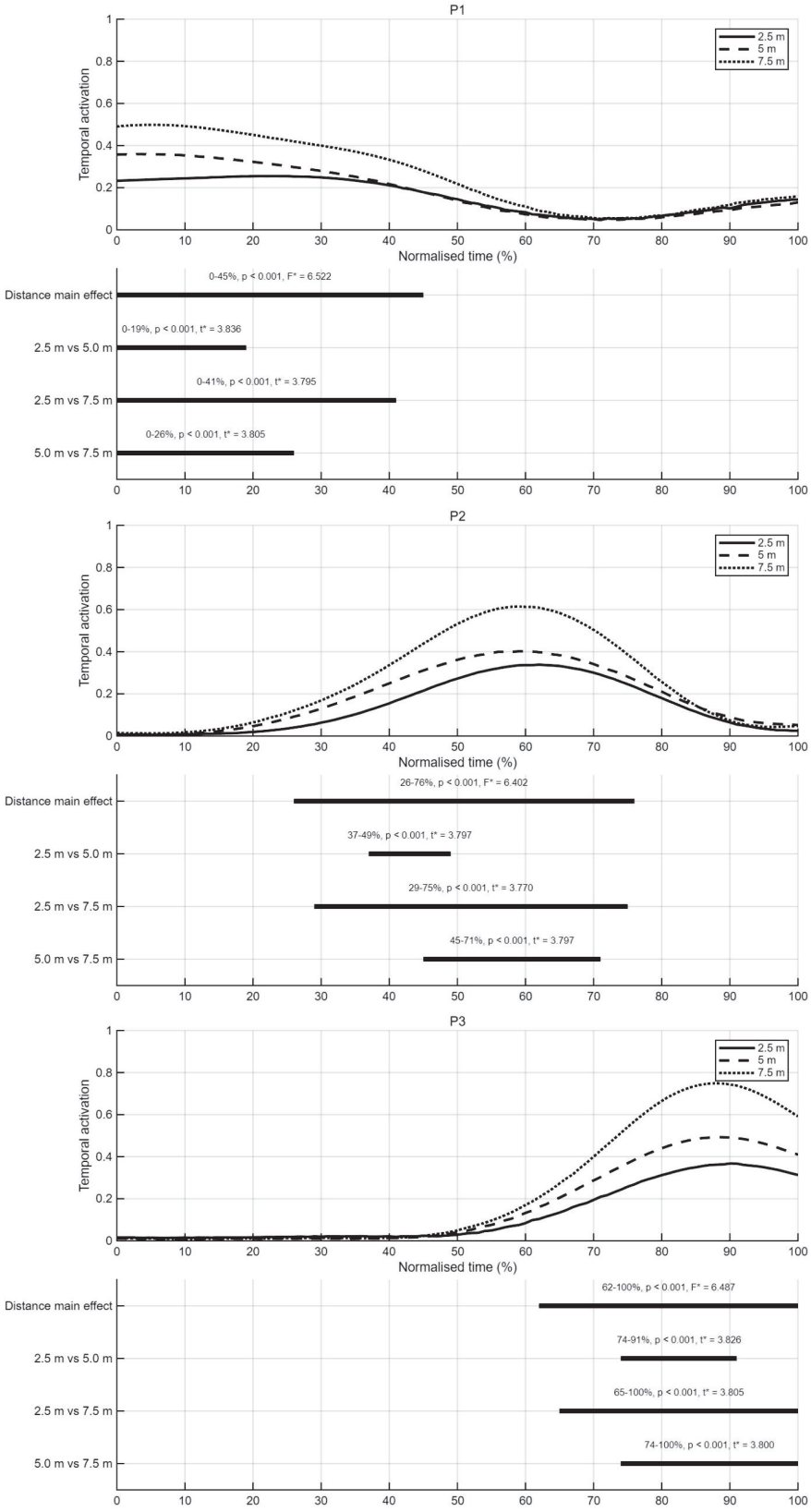

Figure 7. SPM1d one-way repeated-measures ANOVA (RM-ANOVA) examining the effect of passing distance on the three motor primitives (P1–P3). For motor primitives showing a significant distance effect, post hoc pairwise comparisons between distances (2.5 vs 5.0 m, 2.5 vs 7.5 m, and 5.0 vs 7.5 m) are presented; horizontal bars indicate the time intervals with significant differences.

- Copyright - Il Pensiero Scientifico Editore downloaded by IP 18.97.14.82 Wed, 18 Nov 2026, 17:53:39

Table 3. SPM1d results for motor primitives across passing-distance conditions.

Primitive	Test	Comparison	Significant interval (%)	Critical threshold	Cluster p	Mean effect size
P1	SPM(F) RM-ANOVA	Distance main effect	0.0–45.0	F* = 6.510	<0.001	$\eta p^2 = 0.484$
P1	SPM(t)	5.0 m > 2.5 m	0.0–19.0	t* = 3.836	<0.001	dz = 1.015
P1	SPM(t)	7.5 m > 2.5 m	0.0–41.0	t* = 3.795	<0.001	dz = 1.510
P1	SPM(t)	7.5 m > 5.0 m	0.0–26.0	t* = 3.805	<0.001	dz = 0.923
P2	SPM(F) RM-ANOVA	Distance main effect	26.0–76.0	F* = 6.406	<0.001	$\eta p^2 = 0.506$
P2	SPM(t)	5.0 m > 2.5 m	37.0–49.0	t* = 3.797	<0.001	dz = 0.796
P2	SPM(t)	7.5 m > 2.5 m	29.0–75.0	t* = 3.770	<0.001	dz = 1.702
P2	SPM(t)	7.5 m > 5.0 m	45.0–71.0	t* = 3.797	<0.001	dz = 1.336
P3	SPM(F) RM-ANOVA	Distance main effect	62.0–100.0	F* = 6.489	<0.001	$\eta p^2 = 0.602$
P3	SPM(t)	5.0 m > 2.5 m	74.0–91.0	t* = 3.826	<0.001	dz = 1.006
P3	SPM(t)	7.5 m > 2.5 m	65.0–100.0	t* = 3.805	<0.001	dz = 2.154
P3	SPM(t)	7.5 m > 5.0 m	74.0–100.0	t* = 3.800	<0.001	dz = 1.216

Note. F* and t* indicate the critical thresholds for SPM(F) and SPM(t), respectively. Cluster-level p-values refer to the probability values of threshold-surviving significant time intervals obtained from SPM1d random-field-theory inference. Mean ηp^2 and mean dz were computed point-wise and averaged within each significant time interval. Post hoc SPM(t) comparisons were Bonferroni-corrected with $\alpha = 0.017$.

ms, limits opportunities for within-contact temporal adjustment, and the ball is redirected rather than grasped, which constrains online correction during release[6,16]. Under these conditions, preserving a learned temporal template while scaling activation amplitude may provide an efficient solution for increasing ball-flight demands without disrupting release coordination. Together with the distance-dependent reweighting toward greater lower-limb contribution, this preserved temporal organization suggests that distance scaling in overhead passing is achieved through gain modulation within an existing coordination framework rather than through temporal reorganization of motor primitives.

From an applied perspective, the present findings support the use of distance-progressive overhead-passing drills that emphasize whole-body coordination while preserving stable ball-contact and release mechanics. Previous volleyball studies have shown that setting efficacy is closely related to setting technique, tempo, and the quality of the preceding action, highlighting the need to maintain accuracy and timing during training[2]. Biomechanical analyses further indicate that skilled overhead passing depends on coordinated pull–push actions, wrist flexor stretch-shortening behavior, and an elbow-to-wrist kinetic chain during ball contact and release[16]. In addition, proficient setting has been associated with greater concentric force, impulse, rate of force development, and jump height, suggesting that effective setting involves lower-limb force production rather than isolated upper-limb action[34]. Extending these findings, the present synergy-level results indicate that longer passes are achieved mainly by increasing the weightings of lower-limb muscles within existing motor modules, while preserving the overall synergy structure and temporal organization of motor primitives. Therefore, coaches should progress overhead-passing drills from short to long distances while keeping task constraints such as ball height, target accuracy, and release consistency stable. During longer passes, players should be encouraged to generate force from the lower limbs and transfer it through the trunk to the upper limbs, rather than compensating primarily with excessive arm effort. This approach may help players scale passing distance while maintaining the coordination stability and release precision required for effective overhead passing.

Limitations

Several limitations should be acknowledged. First, EMG was recorded from 11 surface muscles representing the upper limb, trunk, and lower limb. Therefore, the extracted synergies may not fully capture the contribution of deeper trunk and hip muscles, which may be important for postural stabilization and force transfer during long-distance passing. Because synergy structure can be influenced by the number and selection of recorded muscles, the present findings should be interpreted as coordination patterns derived from the selected muscle set

- Copyright - Il Pensiero Scientifico Editore downloaded by IP 18.97.14.82 Wed, 18 Nov 2026, 17:53:39

rather than as a complete representation of whole-body neuromuscular control[35]. Second, the extracted synergies may be influenced by EMG processing and model-selection choices, such as normalization, noise removal, filtering, and criteria for selecting the number of synergies[36]. Although the same processing pipeline was applied across all conditions, different methodological choices may yield somewhat different synergy structures or motor primitives. Third, the task was performed under controlled laboratory conditions and did not include match-specific constraints such as locomotion before passing, jump setting, defensive pressure, imperfect reception, or reduced decision time. Finally, because participants were experienced male volleyball players from different playing positions, the findings should be generalized cautiously to elite setters, female athletes, youth players, or athletes with different technical backgrounds.

Conclusions

In conclusion, distance scaling in volleyball overhead passing was achieved mainly through modulation of existing neuromuscular coordination patterns rather than through recruitment of additional synergies. Across the three passing distances, three synergies were consistently identified. As passing distance increased, M1 and M2 showed reweighting toward greater lower-limb contribution, whereas the temporal ordering and peak timing of P1–P3 remained largely preserved. At the same time, motor-primitive activation amplitudes increased with distance, indicating gain modulation within a conserved temporal coordination template. These findings suggest that long-distance overhead passing depends on the ability to amplify and redistribute existing coordination patterns while maintaining release timing. Practically, this supports distance-progressive training that emphasizes whole-body coordination without disrupting technical consistency at ball release.

Conflicts of interest. The authors declare there is no conflict of interest.

References

1. Drikos S, Kouvalias S, Barzouka K. Decoding attack performance: the role of spatiotemporal characteristics in volleyball Complex 1. International Journal of Sports Science & Coaching 2025; 20: 2498-2511.
2. González-Silva J, Domínguez AM, Fernández-Echeverría C, Rabaz FC, Arroyo MP. Analysis of setting efficacy in young male and female volleyball players. J Hum Kinet 2016; 53: 189-200.
3. González-Silva J, Fernández-Echeverría C, Conejero M, Moreno MP. Characteristics of serve, reception and set that determine the setting efficacy in men's volleyball. Front Psychol 2020; 11: 222.
4. Denardi RA, Correa UC, Barros RM, de Oliveira JA, Santos S, Travassos B, et al. The volleyball setter's decision-making on attacking. Int J Perform Anal Sport 2017; 17: 442-57.
5. Dong ML, Ozawa Y, Kitamura S, Chiba I, Inaba Y, Isaka T. The contribution of upper or lower extremity of male athletes differs as distances of overhead volleyball pass increase. J Mens Health 2024; 20: 198-206.
6. Ozawa Y, Dong ML, Kitamura S, Chiba I, Inaba Y, Isaka T. Biomechanical analysis of distance adjustment in volleyball overhead pass. Sports Biomech 2025; 24: 440-57.
7. Okazaki VH, Rodacki AL. Increased distance of shooting on basketball jump shot. J Sports Sci Med 2012; 11: 231-7.
8. Nakano N, Fukashiro S, Yoshioka S. The effect of increased shooting distance on energy flow in basketball jump shot. Sports Biomech 2020; 19: 366-81.
9. Latash ML. The bliss (not the problem) of motor abundance (not redundancy). Exp Brain Res 2012; 217: 1-5.
10. Morasso P. A Vexing question in motor control: the degrees of freedom problem. Front Bioeng Biotechnol 2021; 9: 783501.
11. Berniker M, Jarc A, Bizzi E, Tresch MC. Simplified and effective motor control based on muscle synergies to exploit musculoskeletal dynamics. Proc Natl Acad Sci U S A 2009; 106: 7601-6.
12. Ting LH, McKay JL. Neuromechanics of muscle synergies for posture and movement. Curr Opin Neurobiol 2007; 17: 622-8.
13. Ting LH, Macpherson JM. A limited set of muscle synergies for force control during a postural task. J Neurophysiol 2005; 93: 609-13.
14. d'Avella A, Saltiel P, Bizzi E. Combinations of muscle synergies in the construction of a natural motor behavior. Nat Neurosci 2003; 6: 300-08.
15. Fan P, Feng Y, Jiang C, Zhang X, Long M, Li L, et al. Neuromuscular Control Strategies in Basketball Shooting: Distance-Dependent Analysis of Muscle Synergies. J Sports Sci Med 2024; 23: 571-80.
16. Ozawa Y, Kitamura S, Chiba I, Inaba Y, Isaka T. Biomechanical analysis of volleyball overhead pass. Sports Biomech 2021; 20: 844-57.
17. Li M, Feng Y, Fan P, Zhang X, Jiang C, Li L, et al. Comparing the effects of static stretching alone and in combination with post-activation performance enhancement on squat jump performance at different knee starting angles. J Sports Sci Med 2023; 22: 769-77.
18. Shen B, Wu Y, Tang Y, Mao M, Song Q, Zhang C, et al. Anticipatory COM-COP coordination as a determinant of forehand volley performance in skilled and non-skilled tennis players. Med Sport 2025; 78: 289-98.
19. Dong M, Chiba I, Isaka T, Ozawa Y. Arm slot angles affect elbow and shoulder joint torque in elite college pitchers. Sports Biomech 2025; 24: 2166-83.
20. Kieliba P, Gijt JM, Prado MM, Heinsius J, Sluis RM, Al-Toma AI, et al. How are muscle synergies affected by electromyography pre-processing? IEEE Trans Neural Syst Rehabil Eng 2018; 26: 882 93.
21. Tresch MC, Cheung VC, d'Avella A. Matrix factorization algorithms for the identification of muscle synergies: evaluation on simulated and experimental data sets. J Neurophysiol 2006; 95: 2199-212.
22. Rabbi MF, Pizzolato C, Lloyd DG, Carty CP, Devaprakash D, Diamond LE. Non-negative matrix factorisation is the most appropriate method for extraction of muscle synergies in walking and running. Sci Rep 2020; 10: 8266.

- Copyright - Il Pensiero Scientifico Editore downloaded by IP 18.97.14.82 Wed, 18 Nov 2026, 17:53:39

23. Hagio S, Fukuda M, Kouzaki M. Identification of muscle synergies associated with gait transition in humans. Front Hum Neurosci 2015; 9: 2015.
24. Scano A, Chiavenna O, Malosio M, Molinari Tosatti L, Molteni F. Muscle Synergies-Based Characterization and Clustering of Poststroke Patients in Reaching Movements. Front Bioeng Biotechnol 2017; 5: 62.
25. Cheung VCK, Cheung BHM, Zhang JH, Chan ZYS, Zhou WY, Lau FOH, et al. Plasticity of muscle synergies through fractionation and merging during development and training of human runners. Nat Commun 2020; 11: 4356.
26. Nishida K, Takabayashi T, Nozaki S, Mizutani M, Edama M, Inai T, et al. Comparison of muscle synergies for running between different foot strike patterns. PLoS One 2017; 12: e0171535.
27. Cheung VC, d'Avella A, Tresch MC, Bizzi E. Central and sensory contributions to the activation and organization of muscle synergies during natural motor behaviors. J Neurosci 2005; 25: 6419 34.
28. Pan Z, Wang L, Jiang C, Zhang X, Feng Y, Li L, et al. Characteristics of muscle synergy and anticipatory synergy adjustments strategy when cutting in different angles. Gait Posture 2024; 107: 114-20.
29. d'Avella A, Portone A, Fernandez L, Lacquaniti F. Control of fast-reaching movements by muscle synergy combinations. J Neurosci 2006; 26: 7791-810.
30. Cheung VCK, Seki K. Approaches to revealing the neural basis of muscle synergies: a review and a critique. J Neurophysiol 2021; 125: 1580-97.
31. Kutch JJ, Valero-Cuevas FJ. Challenges and new approaches to proving the existence of muscle synergies of neural origin. PLoS Comput Biol 2012; 8: e1002434.
32. d'Avella A, Bizzi E. Shared and specific muscle synergies in natural motor behaviors. Proc Natl Acad Sci U S A 2005; 102: 3076-81.
33. Overduin SA, d'Avella A, Roh J, Bizzi E. Modulation of muscle synergy recruitment in primate grasping. J Neurosci 2008; 28: 880-92.
34. Cabarkapa DV, Cabarkapa DV, Philipp NM, Eltze A, Whiting SM, Fry AC. Kinetic and Kinematic Characteristics of Setting Motions in Female Volleyball Players. Biomechanics 2022; 2: 538-46.
35. Steele KM, Tresch MC, Perreault EJ. The number and choice of muscles impact the results of muscle synergy analyses. Front Comput Neurosci 2013; 7: 2013.
36. Turpin NA, Uriac S, Dalleau G. How to improve the muscle synergy analysis methodology? Eur J Appl Physiol 2021; 121: 1009-25.

Corresponding author:
Bin Zhu
E-mail: yuebao486@jbnu.ac.kr
Sukwon Kim
E-mail: rockwall@jbnu.ac.kr

- Copyright - Il Pensiero Scientifico Editore downloaded by IP 18.97.14.82 Wed, 18 Nov 2026, 17:53:39

Supplementary Table S1.
Muscle-wise VAF values across synergy numbers and passing-distance conditions.
Values are mean ± SD across 24 participants. VAF = variance accounted for.

Number of modules	Muscle	2.5 m	5.0 m	7.5 m
1	FCR	0.755 ± 0.163	0.728 ± 0.192	0.684 ± 0.147
1	ECU	0.846 ± 0.068	0.820 ± 0.061	0.798 ± 0.092
1	BB	0.822 ± 0.130	0.798 ± 0.142	0.706 ± 0.173
1	TB	0.835 ± 0.104	0.862 ± 0.071	0.883 ± 0.086
1	AD	0.934 ± 0.068	0.926 ± 0.064	0.950 ± 0.034
1	RA	0.872 ± 0.092	0.818 ± 0.116	0.759 ± 0.169
1	ES	0.823 ± 0.134	0.864 ± 0.099	0.853 ± 0.143
1	RF	0.866 ± 0.067	0.770 ± 0.127	0.732 ± 0.118
1	BF	0.848 ± 0.099	0.934 ± 0.053	0.919 ± 0.058
1	GL	0.895 ± 0.064	0.863 ± 0.092	0.885 ± 0.113
1	TA	0.402 ± 0.199	0.324 ± 0.206	0.295 ± 0.140
2	FCR	0.884 ± 0.081	0.856 ± 0.161	0.912 ± 0.096
2	ECU	0.920 ± 0.068	0.924 ± 0.051	0.914 ± 0.063
2	BB	0.917 ± 0.095	0.896 ± 0.097	0.867 ± 0.135
2	TB	0.949 ± 0.058	0.953 ± 0.048	0.939 ± 0.056
2	AD	0.967 ± 0.045	0.967 ± 0.033	0.974 ± 0.027
2	RA	0.932 ± 0.081	0.903 ± 0.091	0.945 ± 0.041
2	ES	0.908 ± 0.113	0.940 ± 0.058	0.947 ± 0.076
2	RF	0.949 ± 0.055	0.901 ± 0.092	0.919 ± 0.091
2	BF	0.931 ± 0.088	0.958 ± 0.038	0.957 ± 0.034
2	GL	0.950 ± 0.031	0.945 ± 0.054	0.974 ± 0.020
2	TA	0.692 ± 0.232	0.644 ± 0.257	0.514 ± 0.259
3	FCR	0.978 ± 0.021	0.958 ± 0.046	0.966 ± 0.044
3	ECU	0.983 ± 0.022	0.969 ± 0.023	0.966 ± 0.030
3	BB	0.971 ± 0.049	0.952 ± 0.059	0.928 ± 0.098
3	TB	0.988 ± 0.017	0.985 ± 0.018	0.979 ± 0.020
3	AD	0.993 ± 0.010	0.987 ± 0.014	0.987 ± 0.017
3	RA	0.969 ± 0.037	0.958 ± 0.044	0.975 ± 0.021
3	ES	0.983 ± 0.015	0.979 ± 0.026	0.980 ± 0.019
3	RF	0.986 ± 0.014	0.966 ± 0.036	0.963 ± 0.040
3	BF	0.984 ± 0.015	0.983 ± 0.021	0.988 ± 0.016
3	GL	0.973 ± 0.027	0.980 ± 0.017	0.991 ± 0.007
3	TA	0.886 ± 0.154	0.908 ± 0.151	0.929 ± 0.111
4	FCR	0.992 ± 0.015	0.989 ± 0.015	0.994 ± 0.009
4	ECU	0.997 ± 0.002	0.993 ± 0.006	0.990 ± 0.015
4	BB	0.994 ± 0.010	0.990 ± 0.010	0.970 ± 0.044
4	TB	0.998 ± 0.004	0.996 ± 0.004	0.996 ± 0.005
4	AD	0.997 ± 0.005	0.998 ± 0.002	0.996 ± 0.004
4	RA	0.986 ± 0.013	0.985 ± 0.019	0.989 ± 0.011
4	ES	0.995 ± 0.007	0.992 ± 0.013	0.993 ± 0.008

Continued

- Copyright - Il Pensiero Scientifico Editore downloaded by IP 18.97.14.82 Wed, 18 Nov 2026, 17:53:39

Supplementary Table S1. Continued.

Number of modules	Muscle	2.5 m	5.0 m	7.5 m
4	RF	0.993 ± 0.010	0.990 ± 0.012	0.994 ± 0.010
4	BF	0.995 ± 0.005	0.995 ± 0.005	0.997 ± 0.004
4	GL	0.992 ± 0.013	0.996 ± 0.005	0.996 ± 0.004
4	TA	0.985 ± 0.018	0.992 ± 0.014	0.995 ± 0.011
5	FCR	0.999 ± 0.000	0.998 ± 0.003	0.999 ± 0.001
5	ECU	0.999 ± 0.002	0.998 ± 0.003	0.998 ± 0.004
5	BB	0.999 ± 0.002	0.998 ± 0.003	0.998 ± 0.004
5	TB	1.000 ± 0.000	0.998 ± 0.004	0.997 ± 0.003
5	AD	1.000 ± 0.001	0.999 ± 0.001	0.999 ± 0.002
5	RA	0.995 ± 0.009	0.996 ± 0.010	0.997 ± 0.006
5	ES	0.998 ± 0.003	0.998 ± 0.003	0.998 ± 0.003
5	RF	0.996 ± 0.008	0.998 ± 0.003	0.999 ± 0.001
5	BF	0.999 ± 0.001	0.997 ± 0.004	0.999 ± 0.001
5	GL	0.998 ± 0.003	0.999 ± 0.003	0.999 ± 0.001
5	TA	0.994 ± 0.010	0.999 ± 0.002	0.999 ± 0.001
6	FCR	0.997 ± 0.010	0.998 ± 0.003	0.999 ± 0.001
6	ECU	0.999 ± 0.003	0.998 ± 0.002	0.997 ± 0.003
6	BB	0.999 ± 0.001	0.998 ± 0.003	0.999 ± 0.002
6	TB	0.999 ± 0.002	0.999 ± 0.001	0.997 ± 0.003
6	AD	1.000 ± 0.001	1.000 ± 0.001	1.000 ± 0.000
6	RA	0.995 ± 0.009	0.998 ± 0.003	0.999 ± 0.001
6	ES	0.999 ± 0.001	0.998 ± 0.003	0.999 ± 0.002
6	RF	0.996 ± 0.008	0.997 ± 0.009	1.000 ± 0.000
6	BF	0.998 ± 0.004	0.998 ± 0.004	0.999 ± 0.001
6	GL	0.998 ± 0.002	0.999 ± 0.001	0.999 ± 0.001
6	TA	0.992 ± 0.025	0.999 ± 0.003	0.999 ± 0.002
7	FCR	0.998 ± 0.003	0.999 ± 0.002	0.999 ± 0.002
7	ECU	0.999 ± 0.001	0.995 ± 0.009	0.995 ± 0.005
7	BB	0.999 ± 0.002	0.998 ± 0.002	0.998 ± 0.003
7	TB	0.999 ± 0.002	0.997 ± 0.004	0.998 ± 0.003
7	AD	0.999 ± 0.003	1.000 ± 0.000	0.999 ± 0.002
7	RA	0.998 ± 0.002	0.998 ± 0.003	0.999 ± 0.001
7	ES	0.998 ± 0.003	0.998 ± 0.004	0.999 ± 0.002
7	RF	0.996 ± 0.006	0.998 ± 0.003	0.993 ± 0.022
7	BF	0.999 ± 0.001	0.998 ± 0.004	0.999 ± 0.001
7	GL	0.998 ± 0.002	0.995 ± 0.011	0.999 ± 0.001
7	TA	0.991 ± 0.021	0.995 ± 0.014	0.993 ± 0.017
8	FCR	0.998 ± 0.003	0.998 ± 0.002	0.994 ± 0.015
8	ECU	0.994 ± 0.020	0.995 ± 0.008	0.992 ± 0.014
8	BB	0.996 ± 0.007	0.998 ± 0.003	0.995 ± 0.014
8	TB	0.996 ± 0.007	0.995 ± 0.011	0.992 ± 0.019

Continued

- Copyright - Il Pensiero Scientifico Editore downloaded by IP 18.97.14.82 Wed, 18 Nov 2026, 17:53:39

Supplementary Table S1. Continued.

Number of modules	Muscle	2.5 m	5.0 m	7.5 m
8	AD	0.998 ± 0.006	0.999 ± 0.002	0.998 ± 0.004
8	RA	0.996 ± 0.005	0.997 ± 0.007	0.994 ± 0.014
8	ES	0.998 ± 0.003	0.998 ± 0.003	0.994 ± 0.011
8	RF	0.996 ± 0.010	0.994 ± 0.013	0.996 ± 0.006
8	BF	0.999 ± 0.002	0.997 ± 0.005	0.999 ± 0.002
8	GL	0.995 ± 0.016	0.993 ± 0.013	0.998 ± 0.006
8	TA	0.992 ± 0.014	0.996 ± 0.008	0.972 ± 0.081
9	FCR	0.985 ± 0.034	0.986 ± 0.047	0.985 ± 0.050
9	ECU	0.992 ± 0.020	0.993 ± 0.011	0.966 ± 0.080
9	BB	0.991 ± 0.029	0.996 ± 0.008	0.978 ± 0.066
9	TB	0.983 ± 0.040	0.995 ± 0.006	0.985 ± 0.027
9	AD	0.996 ± 0.011	0.997 ± 0.005	0.993 ± 0.021
9	RA	0.985 ± 0.020	0.993 ± 0.014	0.988 ± 0.024
9	ES	0.994 ± 0.018	0.997 ± 0.010	0.989 ± 0.028
9	RF	0.980 ± 0.053	0.986 ± 0.040	0.949 ± 0.212
9	BF	0.996 ± 0.006	0.991 ± 0.031	0.988 ± 0.025
9	GL	0.998 ± 0.002	0.991 ± 0.033	0.979 ± 0.085
9	TA	0.971 ± 0.050	0.991 ± 0.016	0.979 ± 0.050
10	FCR	0.990 ± 0.022	0.991 ± 0.021	0.987 ± 0.024
10	ECU	0.985 ± 0.027	0.986 ± 0.023	0.971 ± 0.072
10	BB	0.995 ± 0.009	0.986 ± 0.038	0.987 ± 0.034
10	TB	0.993 ± 0.015	0.993 ± 0.008	0.984 ± 0.030
10	AD	0.998 ± 0.003	0.997 ± 0.006	0.993 ± 0.018
10	RA	0.994 ± 0.011	0.987 ± 0.032	0.985 ± 0.033
10	ES	0.985 ± 0.035	0.964 ± 0.157	0.996 ± 0.008
10	RF	0.992 ± 0.020	0.988 ± 0.045	0.979 ± 0.049
10	BF	0.989 ± 0.032	0.995 ± 0.006	0.992 ± 0.030
10	GL	0.994 ± 0.016	0.987 ± 0.036	0.991 ± 0.024
10	TA	0.920 ± 0.263	0.974 ± 0.107	0.952 ± 0.117
11	FCR	1.000 ± 0.000	1.000 ± 0.000	1.000 ± 0.000
11	ECU	1.000 ± 0.000	1.000 ± 0.000	1.000 ± 0.000
11	BB	1.000 ± 0.000	1.000 ± 0.000	1.000 ± 0.000
11	TB	1.000 ± 0.000	1.000 ± 0.000	1.000 ± 0.000
11	AD	1.000 ± 0.000	1.000 ± 0.000	1.000 ± 0.000
11	RA	1.000 ± 0.000	1.000 ± 0.000	1.000 ± 0.000
11	ES	1.000 ± 0.000	1.000 ± 0.000	1.000 ± 0.000
11	RF	1.000 ± 0.000	1.000 ± 0.000	1.000 ± 0.000
11	BF	1.000 ± 0.000	1.000 ± 0.000	1.000 ± 0.000
11	GL	1.000 ± 0.000	1.000 ± 0.000	1.000 ± 0.000
11	TA	1.000 ± 0.000	1.000 ± 0.000	1.000 ± 0.000

Supplementary Table S2.
Post hoc comparisons of muscle weightings between 2.5 m and 7.5 m

Module	Muscle	2.5 m mean ± SD	7.5 m mean ± SD	Mean difference (7.5–2.5)	95% CI of difference	Test	Raw p	Holm-adjusted p	Effect size	Sig.
M1	BB	0.432 ± 0.240	0.237 ± 0.158	-0.196	[-0.318, -0.073]	paired t-test	0.003	0.024	dz = -0.676	*
M1	AD	0.774 ± 0.338	0.344 ± 0.184	-0.429	[-0.594, -0.265]	paired t-test	<0.001	<0.001	dz = -1.101	***
M1	RF	0.267 ± 0.145	0.744 ± 0.313	0.477	[0.344, 0.611]	paired t-test	<0.001	<0.001	dz = 1.511	***
M1	BF	0.336 ± 0.231	0.623 ± 0.302	0.286	[0.117, 0.455]	paired t-test	0.002	0.017	dz = 0.716	*
M2	FCR	0.289 ± 0.154	0.138 ± 0.102	-0.151	[-0.233, -0.069]	paired t-test	<0.001	0.004	dz = -0.779	**
M2	ECU	1.054 ± 0.436	0.572 ± 0.257	-0.481	[-0.669, -0.294]	paired t-test	<0.001	<0.001	dz = -1.087	***
M2	TB	1.380 ± 0.415	0.851 ± 0.325	-0.529	[-0.774, -0.284]	paired t-test	<0.001	0.001	dz = -0.912	**
M2	AD	1.439 ± 0.379	0.985 ± 0.250	-0.455	[-0.636, -0.273]	paired t-test	<0.001	<0.001	dz = -1.056	***
M2	RF	0.208 ± 0.140	1.333 ± 0.445	1.124	[0.941, 1.308]	Wilcoxon signed-rank	<0.001	<0.001	r = 0.875	***
M2	BF	0.123 ± 0.092	0.313 ± 0.122	0.190	[0.133, 0.246]	paired t-test	<0.001	<0.001	dz = 1.426	***
M2	GL	0.292 ± 0.135	1.273 ± 0.390	0.982	[0.804, 1.159]	paired t-test	<0.001	<0.001	dz = 2.338	***

- Copyright - Il Pensiero Scientifico Editore downloaded by IP 18.97.14.82 Wed, 18 Nov 2026, 17:53:39